Chapter III

Effects of water content and oil on physicochemical and microenvironmental properties of mixed surfactant microemulsions

Abstract

In this report, phase behavior, conductivity, viscosity, dynamic light scattering, fluorescence lifetime, steady state fluorescence anisotropy and Fourier transform infrared spectroscopy (FTIR) techniques were employed for understanding of the physicochemical properties and microenvironment of water-in-oil microemulsion comprising equimolar (1:1) cetyltrimethylammonium bromide (C_{16}TAB) and polyoxyethylene (20) cetyl ether ($C_{16}E_{20}$)/1-butanol/heptane or decane, with varying water content (ω) at 303K. Both conductivity and viscosity of these systems were increased with increase in ω in both oils. Droplet size was also increased with increase in ω and corroborated well with the conductance and viscosity measurements, and depends on oil chain length. The physicochemical changes in the microenvironment with increase in ω were presented by measuring the changes in decay time using a fluoroprobe (7-hydroxycoumarin). The effect of hydration on the microstructure of these systems was studied by polarized fluorescence measurements. FTIR measurements reveal three states of water molecules, viz. trapped, bound and bulk water, in water pool of these systems. Further, the interfacial composition and free energy of transfer of 1-butanol from oil to the interface were evaluated by the dilution method. Changes in interfacial composition as a function of ω corroborate well with FTIR results indicating bound and bulk water.

Keywords: Dynamic light scattering, Conductance, Fluorescence measurement; Fourier transform infrared spectroscopy; State of water; Dilution method.

Colloid Surfaces A., 2014, 450, 130-140

1. Introduction

Microemulsions are ternary or pseudo-ternary dispersed systems comprising mixtures of oil, water and surfactant or (surfactant + cosurfactant). They possess some unique characteristics, such as thermodynamic stability (imparting long shelf-life), compartmentalized polar and non-polar dispersed nano-domains, ease of preparation, low viscosity, ultralow interfacial tension, isotropic and optical transparency (infrequently faint translucency) [1,2]. Due to the existence of both polar and non-polar microdomains, both hydrophilic and lipophilic drug molecules could be solubilized, encapsulated and stabilized in these microscopically heterogeneous and macroscopically homogeneous systems [3]. Typical water-in-oil (w/o) microemulsions or reverse micelles (RMs) consist of nanoscopic water pools dispersed in a nonpolar solvent separated by surfactant monolayer [4]. The physicochemical properties of water molecules localized in the interior of the microemulsions or RMs i.e, confined water is different from those of bulk water, and has been found to be strongly dependent on the chemical nature of the dispersant phase (oil), surfactant, cosurfactant and also on the hydration level of the w/o microemulsions [5, 8]. The change in the structural properties, such as the size, shape, and interfacial rigidity of the microemulsions play an important role in controlling the chemical reactivity of the reactants, morphology of the nano-materials, and the release of the drug molecules from the microemulsion droplets [9-11]. The droplet sizes of the microemulsions are usually controlled by a parameter, ω (which is equal to molar ratio of water and surfactant). Extensive studies have been performed to understand the interaction and dynamics of the microemulsion droplets using various techniques, such as small-angle neutron scattering (SANS), small-angle X-ray scattering (SAXS), transmission electron microscopy, dynamic light scattering (DLS), nuclear magnetic resonance (NMR), fluorescence spectroscopy, conductance, and viscosity measurements [12, 13]. Further, reports on the interaction of dye molecules within confined environment of RMs to elucidate the properties of these organized systems [14, 15]. Dye molecules can be accommodated in a RM in three different locations: (a) external organic solvent, (b) micellar interface formed by surfactant monolayer, and (c) internal polar core depending upon nature of the dye and the medium. Hence, nature and size of RMs can be deciphered by monitoring spectral behavior of dye molecules.

Surfactant mixtures often give rise to enhanced performance over the individual components or exhibit synergism in their physicochemical properties. Because of this property, such mixtures are of theoretical interest as well as could potentially be employed in a wide range of applications. Reports on the use of the blends of ionic/nonionic surfactant microemulsions as templates for enzymatic activity, nanoparticle synthesis, and chemical reactivity are available in literature [16-18]. Further, characterization of water-in oil (w/o) mixed surfactant microemulsions using conductivity [19-21], viscosity [20-22], SANS [23], solubilization [24, 25], interfacial composition [20, 21, 26], Fourier transform infrared (FTIR) spectroscopy [20, 21, 27], and NMR [28] reveals a significant modification of physicochemical properties of the oil/water interface as well as the state of the confined water inside the pool compared to the corresponding single surfactant systems. These findings summarized that the influence of surfactant mixing on overall formation and stability of microemulsions are a direct consequence of molecular interactions of the constituents at the oil/water interface.

Very recently, we have reported the interfacial composition, thermodynamics of alkanol transfer process, solubilization behavior, transport and microstructural properties, and the dynamics of confined water of mixed surfactant (ionic and nonionic) w/o microemulsions under different physicochemical conditions, by employing the dilution method (Schulman's method of cosurfactant titration of the oil/water interface), conductivity, viscosity, DLS and FTIR measurements [20, 21, 25, 26, 29]. In view of these studies, the present report aims at a precise characterization on the basis of molecular interactions among the constituents and explicate the formation vis-à-vis the nature of the oil/ water interface of equimolar (1:1) mixed surfactant w/o microemulsions [water/cetyltrimethylammonium bromide (C_{16}TAB) + polyoxyethylene (20) cetyl ether ($C_{16}E_{20}$)/1-butanol (Bu)/heptane (Hp) or decane (Dc)] as a function of molar ratio of water and surfactant (ω = 10→50) at 303K. Both of these surfactants (C_{16}TAB and $C_{16}E_{20}$) are chosen in such a way that they possess similar hydrocarbon tail (constituting 16 carbon atoms in the linear hydrocarbon chain), but they differ in charge type and size of the polar head groups, so that the possible interaction between the hydrocarbon chains of both surfactants gets minimized [23, 30]. Bu is used as structure making cosurfactant for w/o microemulsion formulation due to its potential industrial as well as biological

applications [31, 32]. Formation, microstructure, internal dynamics (interface dynamics of the droplets and dynamics of confined water) and composition of the mixed interfacial film of these systems have been characterized by means of the phase study, conductivity, viscosity, DLS, fluorescence lifetime, steady state fluorescence anisotropy, FTIR measurements and dilution method as a function of water content. Finally, the correlation of the results in terms of the evaluated physicochemical parameters has been made, which is expected to improve the basic understanding of the formation and characterization of the interface that imparts stability to mixed surfactant w/o microemulsions.

2. Experimental section

2.1. Materials

Cetyltrimethylammonium bromide (C_{16}TAB, >99%), polyoxyethylene (20) cetyl ether ($C_{16}E_{20}$, >98.5%) were the products of Sigma Aldrich, USA and Fluka, Switzerland, respectively. The cosurfactant [1-butanol (Bu, >98%)] and oils [heptane (Hp, >98%) and decane (Dc, >98%)] were products of Fluka, Switzerland, Lancaster, England and E. Merck, Germany, respectively. The dye, 7-hydroxycoumarin (HCM, >99%) and 2-(2,4,5,7-tetrabromo-6-oxido-3-oxo-3H-xanthen-9-yl) benzoate (Eosin Y, >99%) were the products of Chem Service, West Chester, USA and E. Merck, Germany, respectively. Colloidal dispersion of silica (Ludox AM-30 colloidal silica, 30 wt% suspensions in water) was the product of Sigma Aldrich, USA. All these chemicals were used without further purification. Doubly distilled water of conductivity less than 3 $\mu S\ cm^{-1}$ was used in the experiments.

2.2. Methods

2.2.1. Preparation of microemulsion

Microemulsions were prepared using the blends of C_{16}TAB and $C_{16}E_{20}$ at a fixed composition of the surfactant(s) (1:1) in Hp or Dc oil and then adding calculated amount of the de-ionized water or aqueous solution of dye or fluoroprobe(depending upon their solubility's in water) at different concentration levels to obtain the desired ω (= [water]/[surfactant(s)]). The resulting solution was vortexed for about at least 60s. All the samples were single phase and optically transparent under the experimental conditions of the conductance, viscosity, DLS, fluorescence and FTIR spectroscopic measurements reported herein. The addition of the de-ionized water or aqueous dye or fluoroprobe was

controlled by using a micro-syringe. For different instrumental measurements, the composition of the microemulsions was kept constant at mass ratio of surfactant(s) and cosurfactant equals to 1:2.

2.2.2. Phase manifestation

The pseudo ternary phase diagrams of water/(C_{16}TAB + $C_{16}E_{20}$)/Bu/Hp (or, Dc) at equimolar composition (1:1) of mixed surfactants were constructed by titrimetric method. A known amount of mixed surfactants and Bu (1:2, w/w) and oil (Hp or, Dc) or water was taken in a stoppered test tube. Water or oil was then progressively added using a microsyringe under constant stirring in a controlled temperature bath (303±0.1K). The phase boundary was demarcated by the appearance of turbidity, and corresponding composition was noted. The same experiment was carried out for a number of compositions by varying amount of oil or water. It was estimated that the accuracy of the measurements for the transparency-to-turbidity transition was better than ± 2%.

2.2.3. Conductance measurements

Conductivity measurements were made using an automatic temperature-compensated conductivity meter, Mettler Toledo (Switzerland) Conductivity Bridge, with cell constant of 1.0 cm^{-1}. The instrument was calibrated with a standard KCl solution. A constant temperature (303 ± 0.1 K) was maintained by circulating water through the outer jacket from a thermostatically controlled water bath. The reproducibility of the conductance measurement was found to be within ± 1%.

2.2.4. Viscosity measurements

Viscosity measurements were performed using a LVDV-II+PCP cone and plate type rotoviscometer (Brookfield Eng. Lab, USA). The temperature was kept constant (303K) for viscosity measurement within ± 0.1 K by circulating thermostatic water, through a jacketed vessel containing the solution. The reproducibility of the viscosity measurement was found to be within ± 1%.

2.2.5. Dynamic light scattering (DLS) measurements

The size of the microemulsion droplet was determined by DLS method. The same set of solutions, as used for conductance and viscosity measurements, were employed for droplet size analysis at 303K. DLS measurements were carried out using a Zetasizer Nano ZS90 (ZEN3690, Malvern Instruments Ltd, U.K.). A He-Ne laser of 632.8 nm

wavelength was used and the measurements were made at a scattering angle of 90^0. Details of the measurement were presented in our previous reports [20, 21].

2.2.6. Fluorescence lifetime measurements

The fluorescence lifetime measurements were performed at 303K using a bench-top spectrofluorimeter from Photon Technology International (PTI), USA (Model: Quantamaster-40). The present PTI lifetime instrument employs Stroboscopic Technique (Strobe) for time-resolved fluorescence measurements. Fluorescence lifetime of the dye (HCM) was recorded at 450 nm using 310 nano LED as the light source. Instrument response function (IRF) is acquired from a non-fluorescing scattered solution (Herein, Ludox AM-30 colloidal silica, 30 wt% suspension in water) held in a 1 cm path length quartz cell. Analysis has been made by Felix GX (version 2.0) software. Goodness of the fluorescence lifetime data fits of the curves is adjudged by χ^2 value (less than 1.10) and with a residuals trace that is fully symmetrical about the zero axis. Detail of the technique is given in the Appendix A (Sec. 1 and Fig. S1).

2.2.7. Steady state fluorescence anisotropy

Steady state anisotropy (r) was determined using the following expressions [33, 34],

$r = I_{VV} - GI_{VH} / I_{VV} + 2GI_{VH}$ and $G = I_{HV} / I_{HH}$ (1)

where, I_{VV} and I_{VH} are the intensities obtained with the excitation polarizer oriented vertically and the emission polarizer oriented vertically and horizontally respectively; I_{HV} and I_{HH} refer to the similar parameters as above for the horizontal positions of the excitation polarizer. The excitation wave length for probe (Eosin Y) was set at 500 nm (λ_{ex}) and the emission spectra (λ_{em}) were recorded in the range of 500–650 nm [34, 35].

2.2.8. Fourier transform infrared spectroscopy (FTIR) studies

FTIR absorption spectra were recorded in the range of 400-4000 cm^{-1} with a Shimadzu 83000 spectrometer (Japan) using a CaF_2-IR crystal window (Sigma-Aldrich) equipped with a Presslock holder with 100 number scans and spectral resolution of 4 cm^{-1} at 303K. Deconvolution of spectra has been made with the help of Origin software.

2.2.9. The dilution method (Schulman's method of cosurfactant titration at the oil/water interface)

The dilution experiment based on titrimetric method was pioneered by Bowcott et al. [36]. The procedure of this experiment at different physicochemical conditions with

theoretical backgrounds (i.e., basics of the dilution method and evaluation of thermodynamic parameters) were presented in our previous reports [20, 21, 26].

3. Results and discussion

3.1. Phase Behavior of mixed surfactant microemulsions

For the characterization of mixed surfactant microemulsions [water/(C_{16}TAB + $C_{16}E_{20}$)/Bu/Hp (or, Dc)], phase behavior study was undertaken at 303K. A partial phase diagram of the pseudo-ternary systems was constructed by preparing the samples at 57 different compositions for an overview of the phase behavior (i.e. clear microemulsion zone; 1ϕ and biphasic zone; 2ϕ). However, appearance of viscous and other phases along the [surfactant(s): cosurfactant/water]-oil axis have not been shown for simplicity. Determination of the boundaries of the microemulsion region was then refined through a titration process of mixtures of oil (Hp or Dc), surfactant (C_{16}TAB + $C_{16}E_{20}$) and cosurfactant (Bu) (S: CS = 1: 2, w/w) with water by observing transition from clear transparent solution to turbid solution through visual observation. To begin with the titration process, water was added drop wise to an oil/mixed surfactant-cosurfactant blend with a varying amount of oil (100.0 → 0.0 wt %). The findings and the discussions on the phase behavior are presented with the help of phase diagrams in the Appendix A (Sec. 2 and Fig. S2).

3.2. Dynamic light scattering (DLS) studies

DLS measurements have been proved to be a precise and convenient tool for investigating the structural properties of w/o microemulsion systems, as reported by several authors [7, 14, 15, 20, 21, 25, 27, 29, 34]. Herein, the size and size distribution of droplets in w/o microemulsions were characterized by DLS measurements as a function of water content (ω) at 303K. The same experimental path was used, as that of conductivity and viscosity measurements were chosen. All kinds of droplet shapes were imitated to spheres during the DLS measurements. Therefore, the size of the possible globule shape of microemulsion droplet was real dimension or similar to it [37]. Typical values of polydispersity index (PDI) which was calculated according to the International Standard on dynamic light scattering ISO 13321 [38] and was obtained in the range 0.1-0.2. This indicates that the sample is rather monodisperse in nature [39, 40].

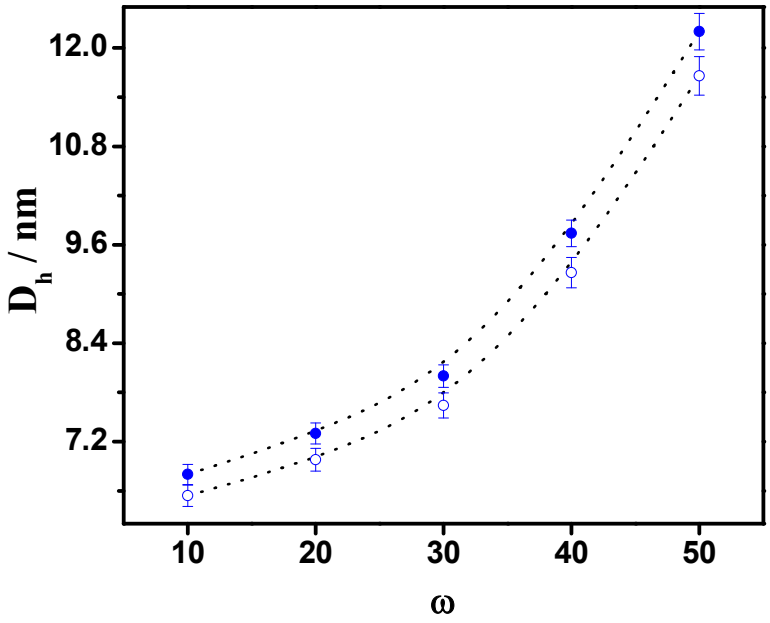

Fig. 1. Hydrodynamic diameter (D_h) of water/(C_{16}TAB + $C_{16}E_{20,}$ 1:1)/Bu/Hp (or Dc) microemulsions as a function of molar ratio of water to surfactant (ω) at a constant temperature of 303K. Open circle: Bu/Hp, filled circle: Bu/Dc. Dotted lines are guide to the eye.

It reveals from DLS measurements, that hydrodynamic diameter (D_h) of the microemulsion droplets increase remarkably from 6.54 nm to 11.66 nm and 6.80 nm to 12.20 nm in Hp and Dc, respectively with the increase in water content (ω = 10→50) in the mixed systems, keeping other parameters constant (Fig. 1). When water is added to dry RMs, a portion of the water goes to the interface and hydrates the head group of surfactants until they reach a maximum, becoming fully hydrated at a certain ω. Additional water then goes primarily to the inner core, leading to continuous increase in the volume of core water with a further increase in ω. This result in a change in the distribution of surfactant molecules to cover the increased volume of water, and subsequently, the smaller droplets are combined into larger ones [41]. These results are consistent with the evaluation of the effect ω on the size of nonylphenylpolyethoxylates (NP)-based RMs stabilized in cyclohexane [41]. Recently, Zhang et al. [42] and Kundu et al. [29] reported similar results for AOT/IPM/alcohol/water and AOT/Tween-85/IPM or IPP or EO/water reverse micelles, respectively.

It can be observed from Fig. 1 that hydrodynamic diameter (D_h) increases with increase in water content (ω) linearly up to a certain ω (~ 30), i.e., swelling of microemulsion droplets has been followed, as it is well established for water or polar solvent/surfactant/oil microemulsions [43]. This feature also demonstrates that the w/o microemulsions consist of discrete spherical and non-interacting droplets of water stabilized by surfactant(s). Deviation from the linearity has been observed beyond $\omega \geq 30$ (Fig. 1). It may be due to several factors. Of these, the most relevant one is the droplet-droplet interaction [43].

Further, it can be observed from Fig. 1 that, droplet size increases with increase in chain length of oil (Hp→Dc) at comparable conditions. Similar observation was also reported in literature [44]. However, an increase in droplet size with increase in ω and oil chain length corroborates well with results obtained from conductance and viscosity measurements, and has been dealt in the Appendix A (Sec. 3, Sec. 4 and Fig. S3 and Fig. S3, inset A).

However, it can be mentioned that DLS gives an estimate of a diffusion coefficient (and hence, a particle size) based on a model shape [7, 15, 21, 27]. Refinement of data pertaining to the droplet size of the microemulsion was done by some authors using pulsed field gradient spin-echo NMR (PGSE-NMR) measurement of diffusion coefficient [45-47]. But, the applicability of NMR technique to the present quaternary mixed microemulsion systems become complicated due to the presence of the alcohol (cosurfactant) in the continuum phase and the size of the microemulsion droplet is not a simple function of ω only [45, 48]. Moreover, the interpretation of the interaction parameter (κ), which is involved in the first term of virial expansion of diffusion coefficient in NMR technique, becomes obscure in the presence of complex hydrodynamic interactions in the present mixed surfactant microemulsion systems [45, 49-51]. Hence, comparatively less complicated and commonly used technique, DLS measurement has been employed for delineation of structural characteristics of these systems. Recently, Bumajdad et al. [52] reported that the droplet size measured by DLS was found to be reasonably similar to that determined by PFG-NMR experiment for water/DDAB/DTAB/n-heptane system.

3.3. Photophysical Studies

In photophysical study of w/o microemulsions or reverse micelles, the choice of photosensitive probe molecule (i.e., fluoroprobe) is important. Compounds with low polarity or high hydrophobicity would reside near the interface, whereas those with high polarity or low hydrophobicity would reside in the polar core of microemulsion droplet [53, 54]. In the present study, neutral fluoroprobe (HCM) and anionic xanthenes dye (Eosin Y) have been chosen as probe(s) for photophysical studies (viz., florescence lifetime and steady state anisotropy measurement) according to their preferential solubility at the interface [53, 54] and polar core of microemulsion, respectively [34, 35]. Recently, the simulation study has revealed that the CTAB molecules are more compressible and ordered in nature at the oil/water interface [55]. The water molecules present in the hydration layer are found to be preferentially distributed in the region between the three partially charged methyl head groups of C_{16}TAB [56]. On the other hand, the hydrophilic head group conformation of polyoxyethelene ether type nonionic surfactant molecules depends on its hydration [57] and form 'all trans' or 'helix conformation in reverse micelles with the network of H-bonding between ether oxygen atom and water [58]. However, overall scenario is much complicated in case of mixed surfactant systems and the unlike interaction (for example, cationic-nonionic interaction) in mixed systems might predominates over the like interaction (for example, ionic-ionic or nonionic-nonionic interactions) in pure micelles upon hydration [59].

3.3.1. Fluorescence lifetime measurement

Fluorescence lifetime study in mixed surfactant w/o microemulsions has been undertaken to obtain information about the configuration of altered interfacial region of the mixed amphiphiles with increase in water content that is, upon hydration ($\omega = 10 \rightarrow 50$), using HCM ($10^{-5}$ mol dm^{-3}) as fluoroprobe [60]. The fluoroprobe (HCM) has been chosen in the present study, because of the fact that the probe mainly resides at the interface and/or faces the polar core upon excitation as reported earlier [53, 54]. Fluorescence lifetime measurement is a highly sensitive imaging method and the lifetime of a fluoroprobe can alter in response to the changes in the conformational state of the fluoroprobe or in response to the interaction with local environment [60]. In the present report, the probe molecules exhibit in two different environments: initially i.e., up to $\omega = 20$ with a large

difference in lifetime of the residing probes, beyond which (ω > 20) a single lifetime value has been displayed. This indicates the presence of all probe molecules in the identical environment at higher ω values (Appendix A, Table S1). For example, the probe molecules exhibit shorter lifespan of 2.56 ns and 2.76 ns along with a longer lifetime of 36.28 ns and 37.51 ns at ω= 10, whereas only shorter lifespan of 4.39 ns and 4.57 ns have been found to exist at ω = 50 for Hp and Dc derived systems, respectively. Generally, interaction with local environment results in fluoroprobe to release the excited state energy faster, leading to a shorter lifespan and vice versa [61]. Hence, in all probabilities, the first kind of probe molecules, i.e., the molecules with shorter lifespan, reside at comparatively complex environment with fairly strong and effective interactions therein (interfacial region where most of the dye molecules are essentially located [53, 54]. On the other hand, the dye molecules with longer lifespan probably exist in quite simple environment in continuous phase. It is interesting to note that these types of probe molecules have not been found with increasing ω (> 20) and the molecules with shorter lifespan only exist. It suggests that the dye molecules are mainly located at the interfacial region with larger surface area of the microemulsion droplet beyond ω = 20 [53, 54].

In the present report, the shorter fluorescence lifetime of HCM (interfacial probe molecules) in mixed microemulsions has been found to influence with the variation in water content all around the experimental range of ω (=10→ 50) (Fig. 2). Thus, by measuring the changes in such lifetime values $\langle\tau\rangle$ with increasing water content, the physicochemical changes in the interfacial microenvironment of w/o mixed systems surrounding the fluoroprobe have been measured indirectly, and a representative plot has been depicted in Fig. 2. It can be observed from Fig. 2 that the lifespan of fluoroprobe $\langle\tau\rangle$ gradually increases from 2.56 ns to 4.95 ns and 2.76 ns to 5.09 ns with the increase in water content up to ω = 40, and then decreases to 4.39 ns and 4.57 ns at ω = 50 for Hp and Dc derived systems, respectively. For w/o microemulsion system, increase in ω leads to decrease in concentration of the surfactant on the droplet surface [65]. It is quite likely that the addition of water to a microemulsion system where mass ratio of surfactant and cosurfactant is fixed, decreases the global composition of the mixtures [water/surfactant(s)/cosurfactant/oil], [65] and subsequently, concentration of the surfactant apparently decreases. Therefore, at higher ω, the interface becomes less

complicated or constrained. Consequently, the fluorescence life time $\langle\tau\rangle$ of HCM is expected to increase in absence of severe interactions. Hence, the increasing trend of $\langle\tau\rangle$ value with increasing ω (= 10→40) indicates the manifestation of the reduction in local interactions as well as native environment surrounding the fluoroprobe at the interface. On the other hand, the drop in $\langle\tau\rangle$ value at ω > 40 may be attributed to the enhanced local field effect around the fluoroprobe with the spreading of long POE chain on the droplet surface [26].

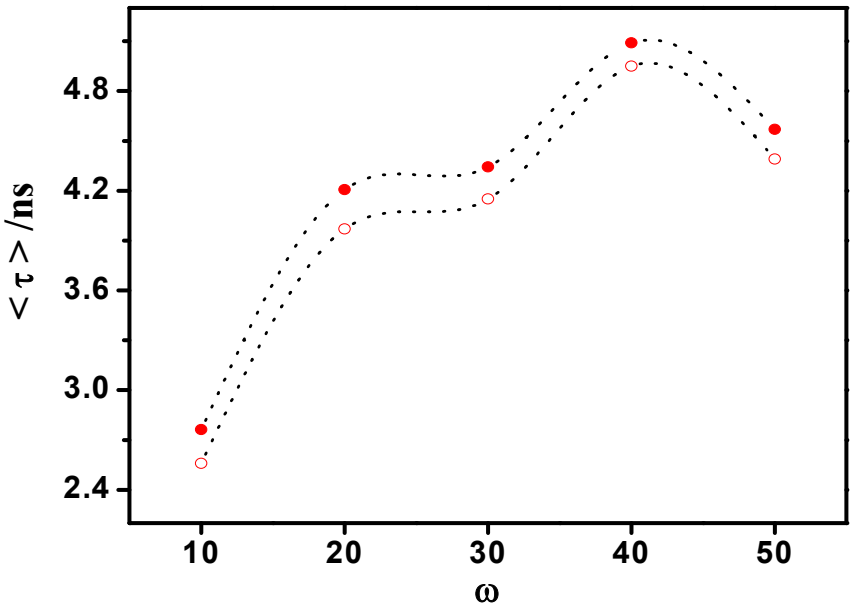

Fig. 2. Fluorescence lifetime of HCM $\langle\tau\rangle$ as a function of molar ratio of water to surfactant (ω) in water/(C_{16}TAB + $C_{16}E_{20,}$ 1:1)/Bu/Hp (or Dc) microemulsions at a constant temperature of 303K, Open circle: Bu/Hp, filled circle: Bu/Dc, Dotted lines are guide to the eye. Representative fluorescence decay of HCM (λ_{ex}= 310 nm) along with corresponding χ^2 values and residual traces have been shown in Appendix A (Sec. 1 and Fig. S1).

It was reported that in nonionic surfactants consisting of POE groups, oxonium ions, that is, positively charged ether oxygen atoms in polyoxyethylene groups of $C_{16}E_{20}$, are so formed in the hydrophilic portion of the surfactants [59, 66]. Hence, it may be concluded

that the polyoxyethylene (POE) chain length is large enough in case of $C_{16}E_{20}$ (i.e., 20 oxyethylene moiety), repulsion exists between the cationic head group [herein, $N(CH_3)_3^+$] and oxonium ions of nonionic surfactant in the mixed systems [59] and induces the spreading of long POE chains on the droplet surface upon hydration ($\omega > 40$) resulting in the observed spectroscopic (fluorescence lifetime and anisotropy) trends of the probe molecules.

However, a slightly higher lifetime has been observed for Dc-derived systems than Hp-derived systems. It has already been evident from DLS measurement that Dc-derived systems depict comparatively larger droplet size than Hp at comparable ω. Hence, the mild drop in population density of surfactant(s) on the droplet surface might be responsible for mild increase in fluorescence lifetime in Dc continuum. Further, comparable $\langle\tau\rangle$ values have been displayed at $\omega = 20$ and 30 (Fig. 2). The transfer of probe molecules from the continuous (oil) phase to the interface through the process of partition completes at $\omega \geq 20$ [as evidenced from bi-exponential to mono-exponential transition of the fluorescence decay curve (Fig. S1)] and further complicates the interfacial region. The similarity of the $\langle\tau\rangle$ values in $\omega = 20 \rightarrow 30$ region, is most probably the result of two mutually opposite effects on the lifetime: increasing tendency due to less constrained interface at higher ω, which is compensated by the enhanced population of the dyes (probes) at the interface. Therefore, the non-monotonic behavior of $\langle\tau\rangle$ as a function of ω can not be accounted for the trend of the droplet size alone, but also other factors, for example, partitioning of various species of a multi-component system in different phases and the modification of the polarity of these phases are also very much involved.

The change in fluorescence lifetime of fluoroprobe $\langle\tau\rangle$ with the variation of ω ($\omega = 10 \rightarrow 40$) for w/o microemulsion is not uncommon in the literature [62, 63]. However, most of these studies focus toward the solvation dynamics of the probe molecules [62, 63]. It may be noted that the size of the water pool increases with increasing ω ($= 10 \rightarrow 50$) and consequently, the dynamics of solvated probe molecules become much faster in these systems. The limited resolution of our nanosecond-resolve instrument is unable to detect the ultra-fast component of solvation dynamics of probe molecules.

Since we are concerned with the consequence of the changes in interfacial composition on the local environment of probe molecules, such deficiency is not expected to affect significantly our conclusions. However, it should be noted that the physicochemical and the photophysical scenarios at the interface as well as polar region of mixed microemulsions are comparatively complex than single surfactant microemulsions.

3.3.2. Steady State Fluorescence Anisotropy

The steady-state anisotropy or polarized fluorescence study provides a simple means of monitoring the processes, wherein the microstructure of the microemulsion is affected in some way [60]. Further, the anisotropy is considered as an index of the microviscosity or rigidity in the microenvironment of the probe [64]. In order to underline the effect of hydration ($\omega = 10 \rightarrow 50$) on the microstructure of the systems under investigation, we have performed polarized fluorescence measurements by using Eosin Y as a fluorescence probe [60]. In view of the present study, the following characteristics features of Eosin Y are important. It is soluble in water, but remains insoluble in n-alkanes. Further, Eosin Y is negatively charged, while the mixed surfactant polar head groups [$(CH_3)_3N^+$ ion of $C_{16}TAB$ and oxonium ion of POE chain of $C_{16}E_{20}$)] are positively charged [59]. Hence, Eosin Y probably locates in the vicinity of palisade layer of the mixed surfactants [35, 67]. Accordingly, the rotational behavior of the probe is expected to provide information about the dynamics of the surfactant molecules in the mixed microemulsion [67]. Actually, the degree of depolarization of the fluorescence emission of a molecular probe is a measure of its rotational diffusion during the excited lifetime [33]. Fluorescence anisotropy (r) is an experimental measurement of the fluorescence depolarization. The lower the anisotropy value, the faster is the rotational diffusion [60].

In highly structured microenvironments, the rotational diffusion of the probe is restrained. Consequently, the probe does not assume all possible orientations with equal probability [33]. However, the objective of the present report is not to determine the absolute values of anisotropy around the probe, rather to evaluate the relative changes in values of anisotropy upon hydration ($\omega = 10 \rightarrow 50$), and a representative plot has been depicted in Appendix A (Fig. S4). It can be observed from Fig. S4 that the anisotropy value of present fluoroprobe (r) (at a concentration of 10^{-5} mol dm^{-3}) gradually decreases from 0.161 to 0.122 and 0.157 to 0.120 with the increase in the water content up to $\omega =$

40, and thereafter, slightly increases to 0.127 and 0.126 at ω = 50 for Hp and Dc derived microemulsion systems, respectively. The interpretation of the results emerges from steady-state anisotropy of these complex microheterogeneous systems is not straightforward, as its value depends on the fluorescence lifetime of the probe, the rotational motion and the possible hindering potential due to the neighboring surfactant molecules [67]. However, a plausible explanation for such variation in anisotropy (r) with water content (ω = 10→50) in the present report is as follows: increase in ω leads to decrease in the surfactant concentration on the droplet surface for w/o microemulsion systems, as discussed in the preceding section (Sec. 3.3.1). Consequently, the packing of the amphiphiles at the interface is less compact (i.e., loosen) with increase in ω and manifests a drop in anisotropy values (faster rotational diffusion) with the formation of less ordered structures up to ω equals to 40 [33, 60]. Thereafter, a mild increase in anisotropy value at ω > 40 probably reflects the spreading of long POE chains on the droplet surface due to repulsion between oxonium ions in polyoxyethylene groups of $C_{16}E_{20}$ and cationic head group [$N(CH_3)_3^+$] of $C_{16}TAB$ [59, 66] with mild enhancement in local interactions [26]. Furthermore, Hp-derived systems show a slightly stronger anisotropic than Dc-derived systems. Similar trend of anisotropy values with increase in ω was reported for water/AOT/heptane (dodecane) systems by Wittouck et al. [67] and Valeur et al. [68] using crystal violet and perylene derivatives as fluorescence probes, respectively.

3.4. Vibrational spectroscopy

In order to get a clear understanding of various interactions in the droplet core, including the type of H-bonding which is operative within the water pool, we employed an excellent and noninvasive technique viz., Fourier transform infrared spectroscopy (FTIR). Several authors have significantly contributed to the understanding of the water dynamics in w/o microemulsion system by studying the state of water using FTIR method [6, 7, 69-73]. The characteristics of the water molecules confined inside the water pool depend strongly on both water content and the nature of the surfactant head group. A detail observation on the dynamics and nature of encapsulated water in AOT reverse micelles with the large variation in water content (ω = 2→60) was reported by Piletic et al. [6] using linear and nonlinear infrared spectroscopy. FTIR study has been carried out

to determine the inherent characteristics of encapsulated water in water/(C_{16}TAB + $C_{16}E_{20}$)/Bu/Hp system at equimolar (1:1) composition under varied ω (= 10→50). It reveals from DLS measurements that the hydrodynamic diameter of droplets (D_h) varies from 6.54 nm to 11.66 nm as a function of ω (= 10→50) for the above system. Reports on using similar range of D_h for studying confined water in microemulsion systems from FTIR measurements are available in literature [69, 71]. Recently, Nickolov et al. [73] and Mehta et al. [72] reported different types of distinguishable hydrogen bonded water molecules in cationic (C_{16}TAB) as well as nonionic (Brij-96) w/o microemulsions stabilized by Bu, respectively. The influence of OH stretching vibration at the Bu site on the intensity of OH stretching of the confined water has been assumed to be insignificantly small and, therefore, ignored in both the cases. In the present study, Bu is used as a structure forming cosurfactant in mixed surfactant microemulsions. However, such an assumption might be a doubtful proposition for the present system. To eliminate the effect of OH stretching vibration at the Bu site on the stretching band of water, the spectra of Bu at the same concentration has been subtracted from the spectral intensity of OH stretching band of water at corresponding ω, and the differential spectra have been analyzed. The final spectra are deconvoluted into three peaks near 3300, 3550 and 3600 cm^{-1} which correspond to OH stretching frequencies of bulk water, bound water and trapped water molecules, respectively [69, 70] and are depicted in Fig. S5 (Appendix A). The bound water molecules are believed to be located in the mixed surfactant's palisade layer, whereas the bulk water exists at the core. The trapped water molecules are present as monomers (without any hydrogen bonding or other linkages with either surfactant or cosurfactant at all) near the long hydrocarbon chains of the surfactant molecules. The relative population of different types of water molecules has been found to be affected with the variation of water content (ω = 10→50) in Bu stabilized w/o mixed microemulsion systems. A representative picture of deconvoluted spectra is depicted in Fig. S5. Corresponding residuals graphs of the deconvolution along with the subsequent statistical parameters (degrees of freedom, coefficient of determination and reduced χ^2) as evaluated form deconvolution software (Origin Lab) in relation to the fitting of curves have been shown in Appendix A (D, E and F of Fig. S6 and Table S2). The variation of Gaussian profiles (area fraction) of the normalized spectra of different water species

(bulk, bound and trapped water) as a function of ω has been shown in Fig. 3A. Since no coupling effect has been considered, precise calculations of fractions of different water species cannot be achieved from the present results [74]. However, the values are used for comparative purpose as a measure of the relative abundance of different water species [72, 74].

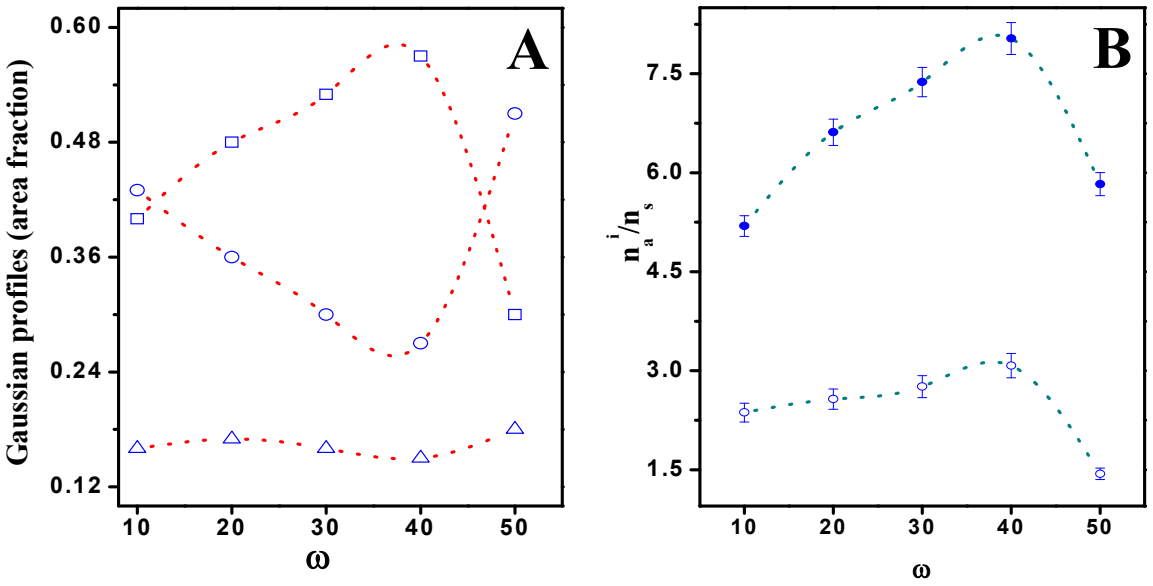

Fig. 3(A) The variation of Gaussian profiles (area fraction) of the normalized spectra (normalized to intensity of 1.0) of different water species (bulk water: open circle, bound water: open square, trapped water: open triangle) as a function of molar ratio of water to surfactant (ω) in water/(C_{16}TAB+$C_{16}E_{20}$, 1:1)/Bu/Hp microemulsions at a constant temperature of 303K. **(B)** Plots of compositional variations of cosurfactant (n_a^i/n_s) (open circle: Bu/Hp, filled circle: Bu/Dc.) vs. molar ratio of water to surfactant (ω) for equimolar (1:1) mixed surfactant (C_{16}TAB and $C_{16}E_{20}$) w/o microemulsion systems comprising 0.5 mmol of mixed surfactant and 14.0 mmol of Hp or Dc oil stabilized by Bu at a constant temperature (303K). Dotted lines are guide to the eye.

It is evident from Fig. S5 and Fig. 3A that bulk water (~ 3300 cm^{-1}) and bound water (~ 3550 cm^{-1}) gradually decreases and increases, respectively with increasing water content up to ω = 40 and thereafter a reverse trend is observed for both bulk and bound water up to ω = 50. The relative population of trapped water molecules remains unaffected with the variation of water content (ω) in these systems. The results are interesting when one considers the various microstructural changes taking place within the isotropic domain of microemulsion. It may be argued that the population of different water species are influenced by charge density of the ionic monomer (herein, C_{16}TAB) [33], the solvation (hydration) of POE head groups of $C_{16}E_{20}$, wherein the head groups [$(CH_3)_3N^+$] of C_{16}TAB reside [75] and the steric compatibility between the two surfactants [33]. At a lower ω, the twisted long POE chains of $C_{16}E_{20}$ molecules might be located covering the head group of C_{16}TAB due to ion-dipole interactions between ionic $(CH_3)_3N^+$ and POE of $C_{16}E_{20}$ [76].

There is an additional scope for the formation of hydrogen bond between penetrated large fractions of POE chains of $C_{16}E_{20}$ and water molecule inside a droplet core. Tasaki [77] reported that a water molecule bridged between POE - oxygen separated by two EO units with hydrogen bonding. The extensive hydrogen bond network was found, running through the POE helix, and thus stabilizing the helix. This type of water, which is bound to EO groups or trapped in coils formed by long POE head groups of nonionic surfactant, represents the bound water. The addition of water in the microemulsion system in the range between ω (= 10-40) hydrates long POE chain of $C_{16}E_{20}$ molecules and leads to the enhancement in bound water fraction and simultaneous decrease in free water fraction. This region was reported to be a micellar-swollen region by several authors [78, 79]. However, after attainment of a specific ω (herein, 40), Brij type of surfactant (herein, $C_{16}E_{20}$) is fully hydrated, and thereby, droplet core accommodates more water molecules. Hence, an increase in population of free or bulk-like water (i.e., having water-water interactions only) has been observed beyond ω = 40 [80]. A schematic representation of variation of different states of water in the confined environment as a function of water content is depicted in Scheme 1. Similarly, Mehta et al. [72] reported that the population

of bound water gradually increases with increase in water content at about ω equals to 33 and thereafter a reverse trend was observed for water/Brij-96/Bu/EO systems.

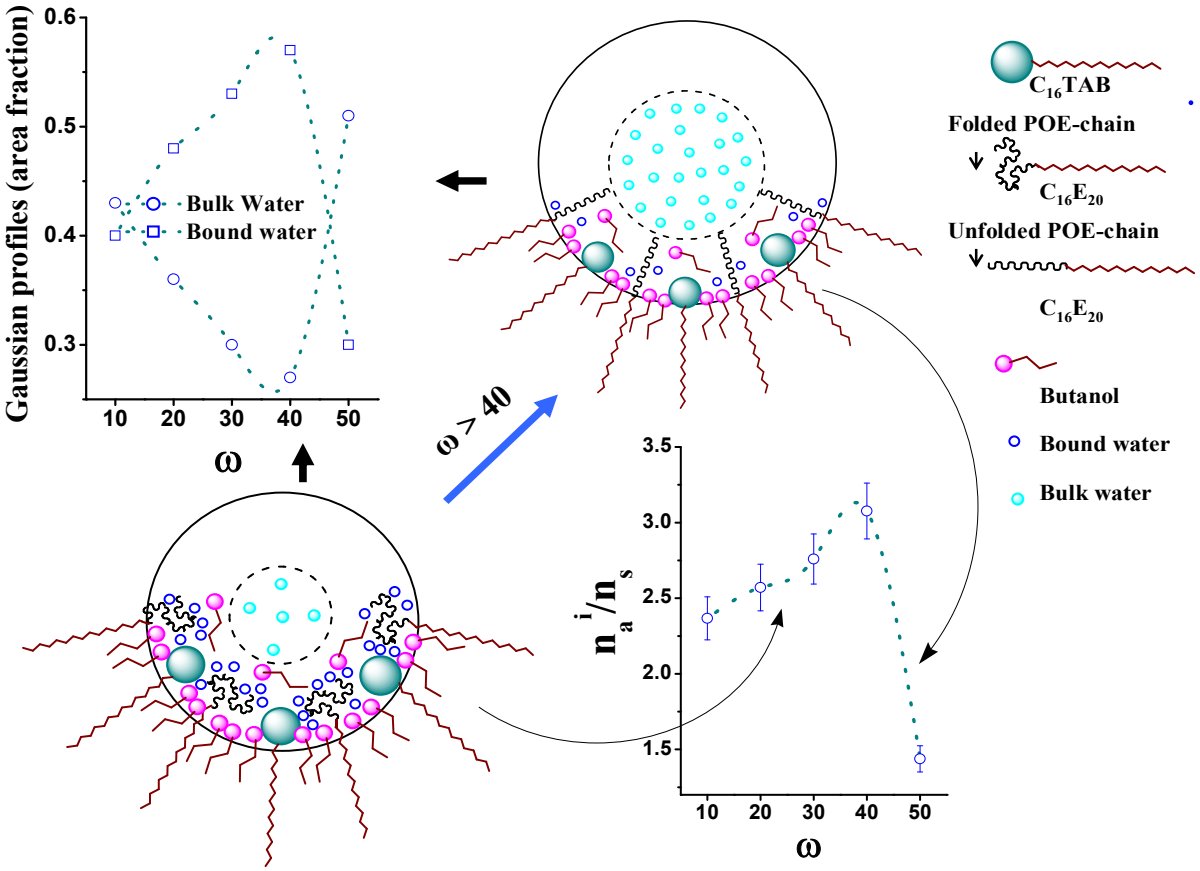

Scheme 1. Schematic representation showing changes in compositional variations at the interface as well as states of water in the pool due to spreading of long POE-chain of $C_{16}E_{20}$ for (w/o) mixed surfactant microemulsion systems [water/(C_{16}TAB + $C_{16}E_{20}$, 1:1)/Bu/Hp] with the variation of molar ratio of water to surfactant, ω (= 10→50).

Further, Jain et al. [79] reported that the enhancement in bound water fraction and a decrease in bulk water in the range between ω equals to 10 and 18 for water/AOT/isooctane systems. The relative population of trapped water molecules has been found to be unaffected with the variation of water content (ω) in these systems. Very recently, Bumajdad et al. [52] reported that solubilized water in reverse aggregates consisting of cationic mixtures with different counter ions (viz. DDAX/DTAX, X = Br^- or Cl^-) in Hp seems to be present as one pseudo-phase, rather than co-existing of

structurally different water layers, as revealed from FTIR and ^{1}H NMR measurements. Further, it was also reported that the presence of mixed surfactants at the interface produces considerable effects on the dynamics of the confined water in mixed AOT/Brij-30/isooctane system, probed by FTIR, adiabatic compressibility and solvation dynamics techniques [7]. To further substantiate these observations, ^{1}H NMR and ultrafast dynamics (picosecond or femtosecond spectroscopy) of confined water molecules in these systems are warranted.

3.5. Estimation of interfacial composition and free energy of transfer process by the dilution method

The w/o microemulsion consists of dispersion of water droplets in Hp or Dc continuum, wherein the mixed surfactants were considered to populate at the oil/water interface in partial association with the cosurfactant (Bu), which distributed between water, the interface and the bulk oil, because of its sparingly water solubility [81]. Thus, at a fixed [surfactant(s)], a critical concentration of Bu is required for the stabilization of the microemulsion. The fundamental basis of the dilution experiment was described in our previous reports [20, 21, 26]. The working equations (detailed derivations are also available in our previous reports [20, 21, 26] and are helpful to rationalize the distribution vis-à-vis transfer process of Bu from the continuous oil phase to the interfacial region:

$$k = n_a^o / n_o \qquad (2)$$

$$\frac{n_a{}^t}{n_s} = \frac{n_a{}^w + n_a{}^i}{n_s} + k\frac{n_o}{n_s} \qquad (3)$$

$$K_d = \frac{X_a{}^i}{X_a{}^o} = \frac{n_a{}^i/(n_a{}^i + n_s)}{n_a{}^o/(n_a{}^o + n_o)} = \frac{n_a{}^i\left(n_a^o + n_o\right)}{n_a{}^o(n_a{}^i + n_s)} \qquad (4)$$

$$\Delta G_t^0 = -RT \ln K_d \qquad (5)$$

where, $n_a^t, n_a^w, n_a^i, n_a^o, n_o, n_s$ denote the total number of moles of alkanol, moles of alkanol in water, at the interface, in the oil phase, the total number of moles of oil and the total number of moles of surfactant, respectively. The distribution constant of alkanol is represented by K_d where X_a^i and X_a^0 are the mole fraction of alkanol in the interfacial layer and in the oil. ΔG^0_t represents standard Gibbs free energy change of transfer of

alkanol from oil to the interface. The data collected from the dilution experiments, graphs were constructed by plotting n_a^t / n_s against n_0 / n_s according to Eq. (3). Representative illustration (at different ω) is depicted in Fig. S7 (Appendix A). Other figures are not exemplified. The plots were strikingly linear (with average R^2 value of 0.9965). The values of n_a^i, n_a^0, K_d and ΔG_t^0, as obtained from Eqs. (3)-(5) are presented in Table 1.

Table 1. Physicochemical parameters for the formation of w/o equimolar (1:1) mixed surfactant microemulsion systems with varying molar ratio of water to surfactant (ω) at afixed temperature (303K).[a, b]

System: water/C_{16}TAB + $C_{16}E_{20}$/Bu/Hp (Dc)					
ω	**10**	**20**	**30**	**40**	**50**
10^4 n_a^i/mol	11.83	12.85	13.79	15.38	7.18
	(25.95)	(33.06)	(36.86)	(40.16)	(29.13)
$10^4 n_a^0$/mol	19.50	27.58	43.55	52.70	58.60
	(52.52)	(67.45)	(82.36)	(92.74)	(108.95)
K_d	11.65	8.65	4.47	3.93	2.82
	(4.05)	(3.46)	(3.03)	(2.82)	(2.43)
$-\Delta G^0_t$/kJ mol^{-1}	6.19	5.43	3.77	3.45	2.61
	(3.52)	(3.13)	(2.79)	(2.61)	(2.23)

[a]All the mixed microemulsion systems are formed using constant amount of mixed surfactant (0.5mmol) and oil (14.0 mmol).

[b] The average errors in K_d and ΔG^0_twere within ±3% and ±5%, respectively.

The plot of compositional variation, n_a^i/n_s (molar ratio of cosurfactant and surfactants at the interface) versus ω for water/C_{16}TAB: $C_{16}E_{20}$ (1:1)/Bu/Hp (Dc) system at 303K, is depicted in Fig. 3B. It reveals from the Table 1 and Fig. 3B that, n_a^i or n_a^i/n_s increases with the increase in ω up to 40 (i.e., reaches a maximum or shows synergism in interfacial composition) and thereafter decreases up to ω = 50 in both oils. Very recently, similar

observation was also reported for water/CPC/Brij-58 or Brij-78/Pn/Hp or Dc microemulsion systems and explained on the basis of molecular interactions of the constituents at the oil/water interface of these systems [26].

A plausible explanation for this type of trend can be presented in the following way. In this report, $C_{16}TAB$ [with $(CH_3)_3N^+$ as polar head group and cetyl (C_{16}) hydrocarbon chain] and $C_{16}E_{20}$ [with polar head group of 20 POE chains and cetyl (C_{16}) hydrocarbon chain] are in a mixed state of equimolar composition. At the threshold level of stability for the formation of w/o mixed surfactant microemulsion, the requirement of Bu depends on physicochemical (molecular) interactions among the constituents [all amphiphiles (viz. $C_{16}E_{20}$, $C_{16}TAB$ and Bu) and water] involved in the microenvironment of the systems. However, molecular interactions may be as follows; electrostatic interaction between polar head groups of ionic surfactant, ion-dipole interaction between polar head groups of ionic and nonionic surfactants, steric interaction between bulky polar head groups of nonionic surfactants and hydrogen bonding interaction between water, and polar head groups of ionic and nonionic surfactants. In the simplest model, two states of water present inside the droplet of w/o microemulsions, i.e., interfacial (or bound) water, which displays modified properties compared with bulk water, and interior (core) water, which behaves similar to bulk or free water [82]. In this model, trapped water which is defined as water species dispersed among long hydrocarbon chains of surfactant molecules with no hydrogen-bonding interaction with its surroundings (discussed in Sec. 3.4), has not been taken into account [83]. The requirement of Bu at the interface gradually increases to fill the gap on large droplet surface and stabilizes the water droplet up to certain ω (herein, ω = 40) due to modification of interfacial (or bound) water and bulk water as a function of ω (discussed in Sec. 3.4). Also, the incorporation of Bu increases due to tighter packing of the surfactant alkyl chains arising out of greater steric compatibility between $C_{16}TAB$ and $C_{16}E_{20}$ [33]. However, after attainment of a specific ω (herein, 40), $C_{16}E_{20}$ is fully hydrated, and thereby, free or bulk-like water (i.e., having only water-water interactions) is formed [80]. Interestingly, this observation is well supported from FTIR measurements (Sec. 3.4), where it has been found that bound and bulk water gradually increases and decreases, respectively with increasing water content up to ω = 40 and thereafter, a reverse trend is observed up to ω = 50. Earlier, it was

reported that the three-dimensional network of water around the nonionic surfactant head group is distorted and thereby detaching the outer weakly associated water layers after a threshold concentration of 1-pentanol for water/$C_{12}EO_8$/1-pentanol/dodecane microemulsion systems [80]. Thereby, with the increase in droplet size by the addition of water, helically twisted POE chain might be unfolded in absence of strong hydrogen bond and it may spread along the surface of the water pool. Thus, it will occupy larger surface area of the droplet and consequently, reduces the free surface area. Hence, mutual accommodation of supporting (or, auxiliary) amphiphile (Bu) with basic (or, major) mixed amphiphiles (C_{16}TAB and $C_{16}E_{20}$) at the interface of fixed amount (n_a^i/n_s) suddenly falls after crossing a certain level of ω (= 40) in both oils. However, overall scenario, as presented above, has been depicted in Scheme 1. Interestingly, this observation corroborates well with the findings from the steady-state fluorescence anisotropy measurements (Sec. 3.3.2), where it has been observed that anisotropy value (r) of the fluoroprobe gradually decreases with the increase in the water content up to ω = 40, and thereafter, slightly increases at ω = 50 as a result of the spreading of long POE chain of $C_{16}E_{20}$ on the droplet surface.

From Table 1, it is clearly evident that n_a^o (number of moles of Bu at the bulk oil phase) increases with increasing ω in both oils. This can be argued as follows. With increasing water content, the interdroplet interaction becomes more attractive and the droplet size increases significantly (Sec. 3.2). As droplet size increases, more oil molecules get accommodated inside the droplet core [26] and thereby n_o increases. In order to maintain constant value of k_o (which equals to n_a^o/n_o) at a given temperature, n_a^o has to be increased, i.e., more Bu molecules require to be solubilized in bulk oil. In this way, n_a^o increases with increase in ω [26, 84]. Similar trend for n_a^o values were also reported earlier for both single and mixed surfactant microemulsions [26, 84, 85].

Further, it is evident from Table 1 that the values of $-\Delta G^0_t$, which is indicative of spontaneity of the alkanol transfer process ($Bu_{oil} \rightarrow Bu_{int}$), decrease with increasing ω (= 10 to 50) for the mixed microemulsion systems. With increasing ω, the relative retention of Bu in bulk oil becomes more than its transfer to the interface (as reflected from values of n_a^o, Table 1). In other words, molecular association between surfactant and cosurfactant molecules at the interface becomes less favorable with increase in ω. Similar

trend of transferring of alkanol (cosurfactant) from oil to the interface and vice versa was reported for single and mixed surfactant microemulsions by Kundu et al. [26], Zheng et al. [84] and Moulik and Hait [85].

In comparison, ΔG^0_t values are more negative in Hp continuum than in Dc, indicating the transfer process to be more favorable (or spontaneous) for the former than the latter. Similar observations were reported by Kundu et al. [26] and Paul and Nandy [86] for w/o microemulsions stabilized by mixed anionic or cationic/nonionic surfactants, as well as single surfactant of different charge types and sizes of the polar head group, respectively. It is quite likely that the interfacial fluidity may increase with increase in oil chain length as well as alcohol partitioning at the interface (n_a^i) (Table 1). Such an increase in interfacial fluidity results in inelastic collisions between droplets, leading to the formation of transient dimmers and an enhanced apparent interdroplet interaction for Dc-based systems. At sufficiently strong interdroplet interaction, the microemulsion droplets stabilized in Dc are less stabilized compared to Hp-based systems [26].

Hence, above discussion on water induced variation in interfacial composition vis-à-vis molecular association of the ingredients at the interface or inside the water pool on the basis of a proposed simple model corroborates well with results of characterization obtained from different experimental techniques presented in previous sections. Such a comprehensive analysis on formation, stability, transport properties, microstructure and microenvironments of mixed surfactant microemulsions has not been reported earlier. However, it should be noted that the physicochemical and the photophysical scenarios at the interface and polar region along with different states of water inside the pool of mixed surfactant microemulsions are comparatively more complex than single surfactant-based microemulsion systems. Further studies in this direction are warranted.

4. Conclusions

The following conclusions can be drawn from the present report.

Phase study reveals a considerable amount of single phase (1ϕ) clear microemulsion zone for mixed systems and has been found to influence by oil chain length. Both the conductance and viscosity gradually increase with increase in ω in both Hp and Dc for the mixed systems, which indicate the enhanced attractive interaction between the

droplets. A sharp enhancement in conductivity at higher water content ($\omega \geq 40$) has been observed due to volume-induced percolation in conductance, which signifies the increase in droplet size, attractive interaction among droplets and exchange rate of materials between the droplets with the addition of water. The hydrodynamic diameter (D_h) of the microemulsion droplets increases remarkably with increase in ω. Further, D_h also increase with increase in chain length of oil (Hp→Dc) at comparable conditions. The increase in droplet size with increase in ω and oil chain length corroborates well with results obtained from conductance and viscosity measurements. It reveals from the fluorescence life time $\langle\tau\rangle$ measurements using HCM as fluoroprobe that $\langle\tau\rangle$ values increase with increasing ω (= 10→40) in both oils. This trend indicates the reduction in local interactions as well as native environment surrounding the fluoroprobe at the interface. Subsequently, drop in $\langle\tau\rangle$ value at $\omega > 40$, may be attributed to the enhanced local field effect around the fluoroprobe with the spreading of long POE chain on the droplet surface. However, Dc-derived systems show a slightly higher lifetime than Hp-derived systems. It has already been evident from DLS measurements that Dc-derived systems show comparatively larger droplet size than Hp at comparable ω. Hence, a mild drop in population density of surfactant on the droplet surface might be responsible for mild increase in fluorescence lifetime in Dc continuum. Further, it reveals from polarized fluorescence measurements using Eosin Y as a fluoroprobe that the anisotropy value (r) of Eosin Y gradually decreases with the increase in the water content up to $\omega = 40$, and thereafter, slightly increases at $\omega = 50$ for Hp and Dc derived systems, respectively, as a result of the spreading of long POE chain of $C_{16}E_{20}$ on the droplet surface. Furthermore, Hp-derived systems show a slightly stronger anisotropic than Dc-derived systems. Additionally, it reveals from vibration spectroscopy measurements that the bulk water (~ 3300 cm^{-1})and bound water (~ 3550 cm^{-1}) have been found to be gradually decreases and increases, respectively with increasing water content up to $\omega = 40$ and thereafter a reverse trend is observed up to $\omega = 50$. The relative population of trapped water molecules remains unaffected with the variation of water content (ω) in these systems. From the dilution method, it has been observed that compositional variation (n_a^i/n_s) increases with the increase in ω up to 40 (i.e., reaches a maximum or synergism) and thereafter, decreases up to $\omega = 50$ in both oils. The trend of water-induced Bu transfer process has

been explained on the basis of the physicochemical (molecular) interactions among the constituents (all amphiphiles and water) involved in the microenvironment of the system and subsequently, results in folding-unfolding of POE chain of $C_{16}E_{20}$ due to variation in bound and bulk like water. The results obtained from the steady-state fluorescence anisotropy and FTIR measurements corroborate well with the model proposed to decipher microstructural rearrangement of the constituents in the microenvironment with variation in water content of these mixed surfactant microemulsions. The spontaneity of Bu transfer process ($Bu_{oil} \rightarrow Bu_{int}$) i.e., $-\Delta G^0_t$, decrease with increasing ω (= 10 to 50) for these systems, which indicates the molecular association between surfactant(s) and cosurfactant molecules at the interface becomes less favorable with increase in ω. Further, changes in compositional variation (n_a^i/n_s) as a function of ω corroborate well with FTIR results.

References

References are given in BIBLIOGRAPHY under Chapter III (pp. 239-243).